

Design local spin models for Gutzwiller-projected parton wave functions

Jia-Wei Mei¹ and Xiao-Gang Wen^{1,2}

¹*Perimeter Institute for Theoretical Physics, Waterloo, Ontario, N2L 2Y5 Canada*

²*Department of Physics, Massachusetts Institute of Technology, Cambridge, Massachusetts 02139, USA*

(Dated: July 4, 2014)

We introduce a method to design a local spin Hamiltonian to realize a Gutzwiller-projected parton wave functions (GPWF) as its ground state. For example, the Dirac spin liquid (DSL) state is quite close to the true ground state of the spin-1/2 Heisenberg model on kagome lattice. We examine what kind of perturbations we should add in order to drive the DSL to more stable chiral spin liquid (CSL), valence bond solid (VBS) or Gutzwiller-projected spin Hall (GSH) states. We compute the two-body reduced-density-matrices (2-RDM) of GPWFs for those target states, and compare them to the 2-RDM of the DSL. This allows us to design local spin models with only two-body interactions that may realize those interesting target states. Our results agree very well with recent numerical calculations for CSL on kagome lattice. We also study spin-1 systems on kagome lattice, and design local spin models that may realize CSL, VBS and symmetry-protected topological (SPT) states. Our work establishes a directional guide for further numerical simulations.

Quantum entanglement has been becoming an important concept to understand and classify the quantum many-body system. It precisely rephrases “topological order” as long-range entanglement.[1, 2] The topological ordered state is not smoothly connected to a direct product state by any local unitary transformation.[3] It has new topological quantum numbers, such as non-trivial ground state structures and fractional excitations.[4–9] In the presence of symmetry, symmetry-protected topological (SPT) state, although short-range entangled, cannot be locally deformed into a direct product state via local unitary transformations that preserve the symmetry.[10–12] Several exactly solvable lattice models are constructed to realize topological orders[13–16] and SPT states[17, 18]. Kitaev *XYZ* model on the honeycomb lattice[13] is an elegant example to use spin Hamiltonian with only two-body interactions to realize a particular topologically ordered state. However, it is a challenging task to find an exactly solvable local spin model that has a generic topologically ordered or a SPT ordered ground state. For a two-dimensional (2D) spin model that is not exactly soluble, expensive numerical methods, e.g., exact diagonalization (ED)[19], projected entangled pair states (PEPS) or tensor-network[20] and density matrix renormalization group (DMRG)[21], are required to access the ground state.

On the other hand, Gutzwiller projective parton construction is a powerful theoretical approach, that allows us to construct the wave functions of many interesting and highly non-trivial topological states for strongly correlated bosonic or spin systems.[22–25] In this letter, we will make a good use of those rich results. We will carry out a reverse engineering: to design a local spin Hamiltonian that realize those topological states described by Gutzwiller-projected parton wave functions (GPWF).

Kitaev *XYZ* spin model[13] and Wen plaquette model[14] are special examples, in which the exact ground states are given by GPWFs. For a general

GPWF, we might be able to find a very complicated Hamiltonian so that the GPWF is the exact ground state. However, real spin systems in general only have strong two-body interactions. In this paper, we will try to design a model Hamiltonian with only two-body interactions, which may optimally realize a interesting GPWF as the ground state.

To design the two-body Hamiltonian, we investigate two-body reduced-density-matrix (2-RDM) of GPWFs. We trace out all configurations except states on two sites of local links, e.g., nearest neighbor (NN), second NN (2NN) and third NN (3NN) bonds. If the 2-RDMs contain sectors with small weights (small eigenvalues), it implies that the GPWF is not frustrated for two-body interactions, and we can design a two-body Hamiltonian to project out those low-weight sectors. The designed Hamiltonian may realize the GPWF as its ground state. The similar idea can be found in the AKLT model construction[26], where the spin-2 sector in 2-RDM has a vanishing weight and is projected out by the designed Hamiltonian.

In this letter, we will take a slightly different approach. We will start with a Dirac spin liquid (DSL) state which is known to be close to the ground state of a simple spin model. We then try to design a perturbation to the original model that may optimally drive the DSL to a more stable state in its neighbor where the Dirac points are gapped.

The π -flux state is an extensively studied DSL for the spin-1/2 system on the 2D square lattice.[27] It is the parent state of many different kinds of states (e.g., antiferromagnetic, *d*-wave superconducting and pseudogap states) in high T_c cuprates.[28] DSL is proposed to be the ground state of spin-1/2 Heisenberg model on the Kagome lattice.[29] Different DSL states are also constructed on the honeycomb lattice.[30–32]

To design a perturbation that drives the DSL to one of its neighbors, we compute the 2-RDMs on several bonds

for both DSL and its neighbor. If the two 2-RDMs are about the same on a bond, then the two-body interaction on that bond will not be helpful to drive the DSL to its neighbor. On the other hand, if the two 2-RDMs are different for some bonds, then, we can design a two-body perturbation on that bond to favor the neighboring state. In particular, if the 2-RDM for the neighboring state has more weight in the high weight sector and less weight in the low weight sector, it will imply that the neighboring state is less frustrated for the designed two-body Hamiltonian, and is likely to be realized.

We apply such an approach to DSL states on kagome lattice for spin-1/2 SU(2) and spin-1 SU(3) systems. The DSL states are very close to the ground states for SU(N) ($N = 2, 3$) spin Hamiltonians with only J_1 term on NN bonds in Eq.(2). We want to drive the DSL to the chiral spin liquid (CSL), valence bond solid (VBS) and Gutzwiller-projected spin Hall (GSH) for spin-1/2 systems, and to CSL, VBS and SPT states for spin-1 systems, respectively. From the variations of 2-RDM, we design the possible local spin models for those states.

The SU(N) spin operator S_β^α has the parton (Schwinger-fermion) representation, $S_\beta^\alpha(i) = f_{i\alpha}^\dagger f_{i\beta}$. Here $f_{i\alpha}$ is the fermionic parton operator on i -site on the lattice and $\alpha = 1, 2, \dots, N$ is the spin (flavor) index. On every site we have the single-occupation constraint, $\sum_\alpha f_\alpha^\dagger(i) f_\alpha(i) = 1$. The GPWF is written as $|\Psi_G\rangle = \sum_{\{R\}} \psi(\{R\}) |\{R\}\rangle$, where the determinate $\psi(\{R\})$ is the wave amplitude for spin (flavor) configuration basis $|\{R\}\rangle$ on the lattice in the ground state of the mean field Hamiltonian, $H_{MF} = \sum_{\langle ij \rangle} (t_{ij}^\alpha f_{i\alpha}^\dagger f_{j\alpha} + u_{ij}^{\alpha\beta} f_{i\alpha}^\dagger f_{j\beta}^\dagger) + \text{H.C.}$. By definition, 2-RDM on sites i and j is written as

$$\rho(ij) = \text{tr}'_{\{R\}} |\Psi_G\rangle \langle \Psi_G| = \sum_{\{ij\}, \{ij\}'} |\{ij\}\rangle \langle \{ij\}'| \frac{\sum_{\{R\}} \psi^*(\{ij\}' \otimes \{R\}) / \{ij\}^R \delta_{\{ij\}, \{ij\}^R} |\psi(\{R\})|^2}{\psi^*(\{R\})}, \quad (1)$$

where $\{ij\}$ is the spin configuration on sites i and j . tr' is the trace running over all spin configurations except two states on sites i and j . $\{ij\}' \otimes \{R\} / \{ij\}^R$ is the configuration by replacing $\{ij\}^R$ in $\{R\}$ by $\{ij\}'$. 2-RDM can be simulated by using the standard Monte Carlo method according to the weight $|\psi(\{R\})|^2$.

DSL has $u_{ij} = 0$ in the mean field Hamiltonian. The complex phase of t_{ij} brings a flux pattern for the parton hopping on the lattice. SU(2) DSL has π flux in the square plaquette on the square lattice and in the hexagon on the kagome lattice, respectively.[27, 29] There is also π flux in the hexagon for SU(4) DSL on the honeycomb lattice.[32] Flux is zero for SU(2) and SU(3) DSL states on the honeycomb lattice[30, 31] and kagome lattice, respectively. The 2-RDM of DSL states has the SU(N) anti-symmetric representation \square and symmetric one \square with the dimensions $\frac{N(N-1)}{2}$ and $\frac{N(N+1)}{2}$, respec-

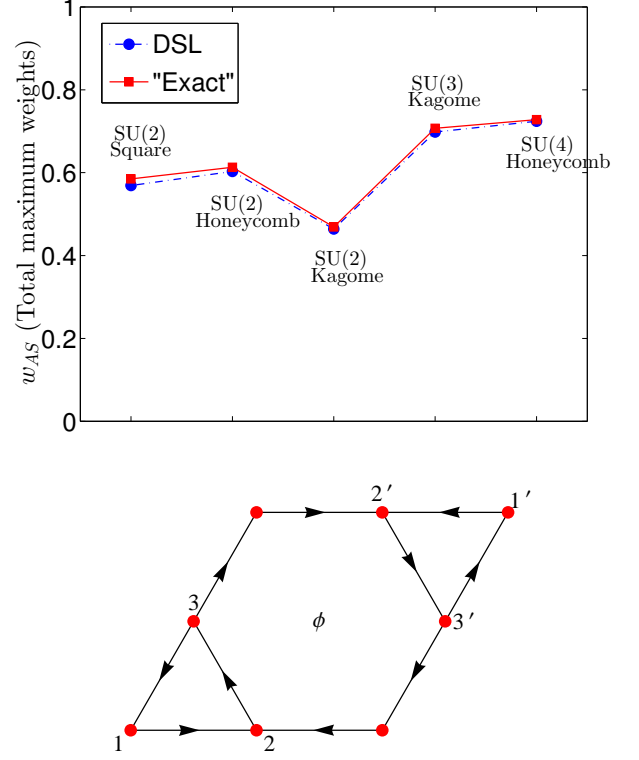


FIG. 1. (a). The anti-symmetric sector (AS) of 2-RDM has $\frac{N(N-1)}{2}$ -fold degenerate maximum weights. The total maximum weights w_{AS} on NN bonds are shown here. Blue solid circles are Monte Carlo results for different SU(N) DSL states on different lattices; red solid squares are extracted from the numerical "exact" ground state energies of J_1 SU(N) models, e.g., SU(2) on the square lattice[33], honeycomb lattice[31], kagome lattice[34] and SU(3) on the kagome lattice[35] and SU(4) on the honeycomb lattice.[32] (b). The kagome lattice. The NN bonds (e.g., $\langle 12 \rangle$) are defined as the sides of triangles \triangle_{123} and $\nabla_{1'2'3'}$. 2NN (e.g., $\langle\langle 23' \rangle\rangle$) and 3NN (e.g., $\langle\langle\langle 22' \rangle\rangle\rangle$) bonds are in the hexagon.

tively. We use the notations, $w_{AS} = \sum_{i=1}^{N(N-1)/2} w_{AS}^i$ and $w_S = \sum_{i=1}^{N(N+1)/2} w_S^i$, for total anti-symmetric and symmetric weights, respectively. The normalization is $w_{AS} + w_S = 1$. w_{AS} is dominant in 2-RDM on NN bonds for these DSL states as shown in Fig. 1 (a).

The SU(N) spin model on the 2D lattice is written as

$$H_0 = J_1 \sum_{\langle ij \rangle} P_{ij} + J_2 \sum_{\langle\langle ij \rangle\rangle} P_{ij} + J_3 \sum_{\langle\langle\langle ij \rangle\rangle\rangle} P_{ij} + \dots, \quad (2)$$

where J_1 , J_2 and J_3 are exchange couplings on NN, 2NN and 3NN bonds. P_{ij} is the SU(N) permutation operator, $P_{ij} = S_\beta^\alpha(i) S_\alpha^\beta(j)$, which swaps two quantum states on bonds. In Fig. 1 (a), we collect some numerical results of w_{AS} of 2-RDM on NN bonds for ground states of SU(N) J_1 spin model, where $w_{AS} = (1 - E_b^1/J_1)/2$ with E_b^1 the ground state energy. DSL states are close to ground states of SU(N) J_1 spin models as seen in Fig. 1 (a).

The mean field Hamiltonian of SU(2) DSL on the kagome lattice is written as

$$H_{\text{DSL}} = -t \sum_{\langle ij \rangle_{\alpha}} e^{i\varphi_{ij}} f_{i\alpha}^{\dagger} f_{j\alpha} + \text{h.c.}, \quad (3)$$

where φ_{ij} brings π flux in the hexagon and zero flux in triangles \triangle_{123} and $\nabla_{1'2'3'}$. The CSL state is obtained by adding extra phase θ on the directed links on kagome lattice (Fig. 1 (b)). The fluxes are now 3θ in triangles \triangle_{123} and $\nabla_{1'2'3'}$ and $\pi - 6\theta$ in the hexagon. With $\theta = 0$ fixed, the VBS state is obtained by varying the ratio of hopping amplitudes t_2/t_1 , where t_1 and t_2 are for bonds on triangles \triangle_{123} and $\nabla_{1'2'3'}$, respectively.

The anti-symmetric (singlet) weight of 2-RDM for the SU(2) DSL is $w_{\text{AS}}^0(\text{NN}) = 0.4645(6)$, $w_{\text{AS}}^0(2\text{NN}) = 0.261(1)$, $w_{\text{AS}}^0(3\text{NN}) = 0.233(2)$. Both CSL and VBS states have the SU(2) spin rotation symmetry. With increasing wave function parameters (θ or t_2/t_1), the responses of 2-RDM on different bonds for different states, $\Delta w_{\text{AS}} = w_{\text{AS}} - w_{\text{AS}}^0$, behave differently as shown in Fig. 2.

w_{AS} of CSL on 3NN bonds is very sensitive to the variation of θ and reaches the maximum at $\theta_c = \pi/6$ where the gap in the mean field Hamiltonian is largest. Meanwhile, VBS is not sensitive to the variation of t_2/t_1 . Since w_{AS} of CSL increases significantly on 3NN bonds as varying θ , we can add J_3 term to the spin model to stabilize the CSL state. The spin-1/2 SU(2) permutation operator is the Heisenberg term, $P_{ij}^{S=1/2} = 2(\mathbf{S}_i \cdot \mathbf{S}_j + \frac{1}{4})$. CSL is the potential ground state for J_1 - J_3 Heisenberg model on the kagome lattice. The estimated critical J_3 is around $J_3/J_1 > 0.3$. The CSL state was already found in DMRG results on J_1 - J_2 - J_3 Heisenberg model on the kagome lattice in Refs. 36 and 37. J_2 term on 2NN bonds is also included in Refs. 36 and 37. From the variation of 2-RDM, J_2 term is not important (even not favored) for the CSL state.

A planar anti-ferromagnetic state can be modeled as the GSH state with the mean field Hamiltonian[38]

$$H = -t \sum_{\langle ij \rangle} e^{i\phi_{ij} + i\theta_{\alpha}} f_{i\alpha}^{\dagger} f_{j\alpha} + \text{h.c.}, \quad (4)$$

where different flavors see opposite flux, $\theta_1 = -\theta_2 = \theta$. 2-RDM of GSH has two independent components of 2-RDM, $\rho_{|11\rangle\langle 11|} = \rho_{|22\rangle\langle 22|}$ and $\rho_{|12\rangle\langle 21|}$. The notations for variations of 2-RDM are as follows

$$\begin{aligned} \Delta\rho_{|11\rangle\langle 11|} &= -(\rho_{|11\rangle\langle 11|} - \rho_{|11\rangle\langle 11|}^0), \\ \Delta|\rho_{|12\rangle\langle 21|}| &= |\rho_{|12\rangle\langle 21|} - \rho_{|12\rangle\langle 21|}^0|, \\ \delta\phi &= \arg(-\rho_{|12\rangle\langle 21|}). \end{aligned} \quad (5)$$

$\rho_{|11\rangle\langle 11|}^0 = 0.1786(2)$, $\rho_{|12\rangle\langle 21|}^0 = -0.143(1)$ are the components of 2-RDM for the reference DSL state. $\rho_{|12\rangle\langle 21|} = -|\rho_{|12\rangle\langle 21|}|e^{i\delta\phi}$ is complex. The variation of 2-RDM for

GSH is shown in Fig. 3. $\Delta|\rho_{|12\rangle\langle 21|}|$ increases significantly with increasing θ . So GSH is favored by the twisted permutation term

$$H^{\text{GSH}} = \sum_{\langle ij \rangle} P'_{ij}, \quad P'_{ij} = S_{\beta}^{\alpha}(i) S_{\alpha}^{\beta}(j) e^{i\Theta_{\alpha\beta}}, \quad (6)$$

with $\Theta_{12} = -\Theta_{21}$ on NN bonds on kagome lattice. In terms of spin-1/2 spin operators, the twisted permutation operator contains Dzyaloshinskii-Moriya (DM) interaction. GSH has a planar spin order. With large DM interactions, the spin order was already found in Ref. 39 for spin-1/2 systems on the kagome lattice.

The spin-1 SU(3) DSL on the kagome lattice has no

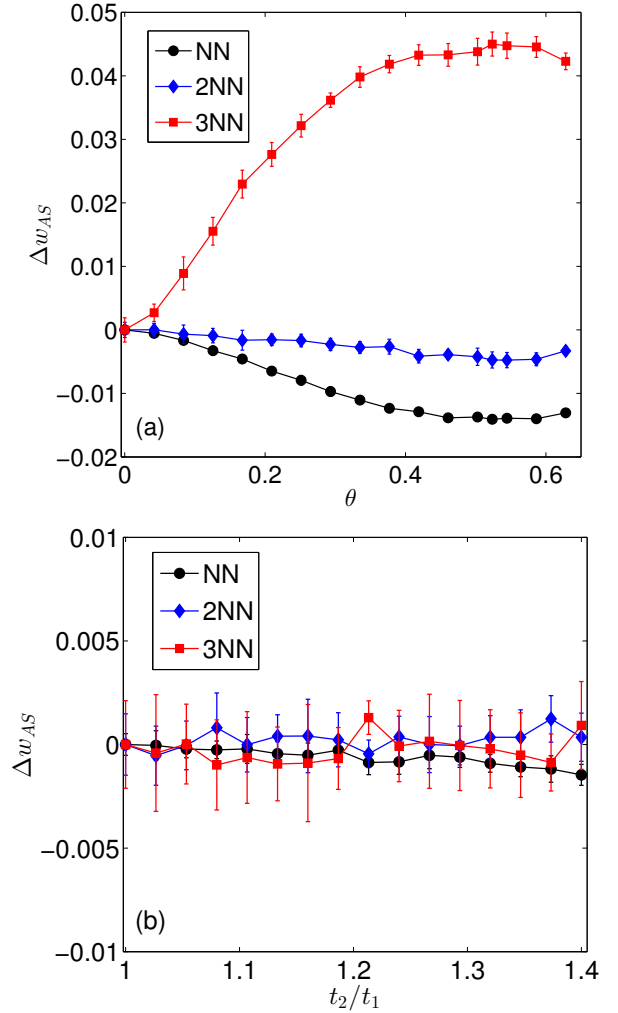


FIG. 2. θ and t_2/t_1 -dependent variations of total maximum anti-symmetric weights $\Delta w_{\text{AS}} = w_{\text{AS}} - w_{\text{AS}}^0$ for SU(2) CSL (a) and VBS (b), respectively, on NN, 2NN and 3NN bonds. $\Delta w_{\text{AS}} > 0$ for SU(2) CSL increases significantly only on 3NN bonds with varying the wave function parameter θ . So only J_3 spin term on 3NN bonds can favor CSL, which agrees very well with Refs. 36 and 37.

flux in the mean field Hamiltonian

$$H_{\text{DSL}} = -t \sum_{\langle ij \rangle \alpha} f_{i\alpha}^\dagger f_{j\alpha} + \text{h.c.}, \quad (7)$$

The SU(3) CSL state has the flux 3θ in triangles \triangle_{123} and $\nabla_{1'2'3'}$ and -6θ in the hexagon; with $\theta = 0$ fixed, we can get the VBS state by varying the ratio of hopping amplitudes t_2/t_1 .

SU(3) DSL state has 2-RDM of weights $w_{\text{AS}}^0(\text{NN}) = 0.694(1)$, $w_{\text{AS}}^0(2\text{NN}) = 0.255(2)$, $w_{\text{AS}}^0(3\text{NN}) = 0.405(3)$. With increasing parameters (θ or t_2/t_1), the responses of 2-RDM, $\Delta w_{\text{AS}} = w_{\text{AS}} - w_{\text{AS}}^0$ are shown in Fig. 4. The nonmonotonicity of $\Delta w_{\text{AS}}(\text{NN})$ for VBS suggests that the NN SU(3) spin model has the stability towards to the VBS state, consistent with the tensor-network numerical calculation.[35] At $t_2/t_1 = 1.125$, VBS has $w_{\text{AS}}(\text{NN}) = 0.7025(4)$. The variational energy per bond $E_b^{\text{VBS}} = -0.4051(8)J_1$ very close to ground state energy in tensor-network simulation, $E_g \simeq -0.415J_1$. [35] Both CSL and VBS states are favored by J_2 SU(3) term on 2NN bonds. When $J_2/J_1 > 0.75$, CSL state is the more likely favored state for the SU(3) spin model.

For spin-1 systems, the permutation operator also contains the biquadratic term, $P_{ij}^{S=1} = \mathbf{S}_i \cdot \mathbf{S}_j + (\mathbf{S}_i \cdot \mathbf{S}_j)^2$. In real materials, the biquadratic coupling is small and the Heisenberg term dominates[40], far away from SU(3) limit. However, theoretically we can still take SU(3) DSL as the reference and turn on the paring of partons to go back to SO(3) symmetry.[41]

The mean field Hamiltonian of SPT is written as[25]

$$H = -t \sum_{\langle ij \rangle} e^{i\theta_\alpha} f_{i\alpha}^\dagger f_{j\alpha} + \text{h.c.}, \quad (8)$$

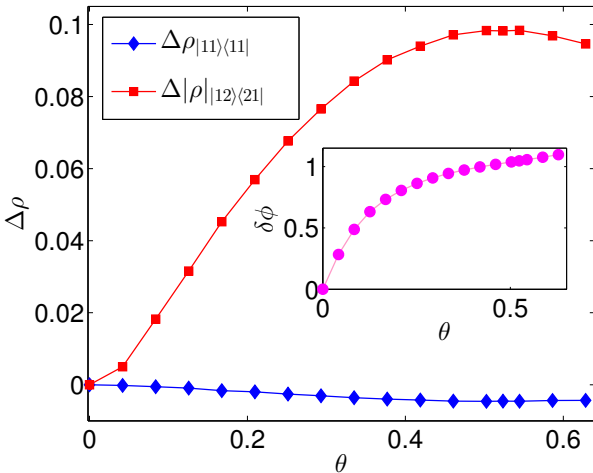


FIG. 3. The θ -dependence of variations of 2-RDM for the GSH state on NN bonds is defined in Eq. (5). The amplitude $|\rho_{|12\rangle\langle 21|}$ and phase $\delta\phi$ increase significantly implying that GSH is stabilized by DM interactions.[39]

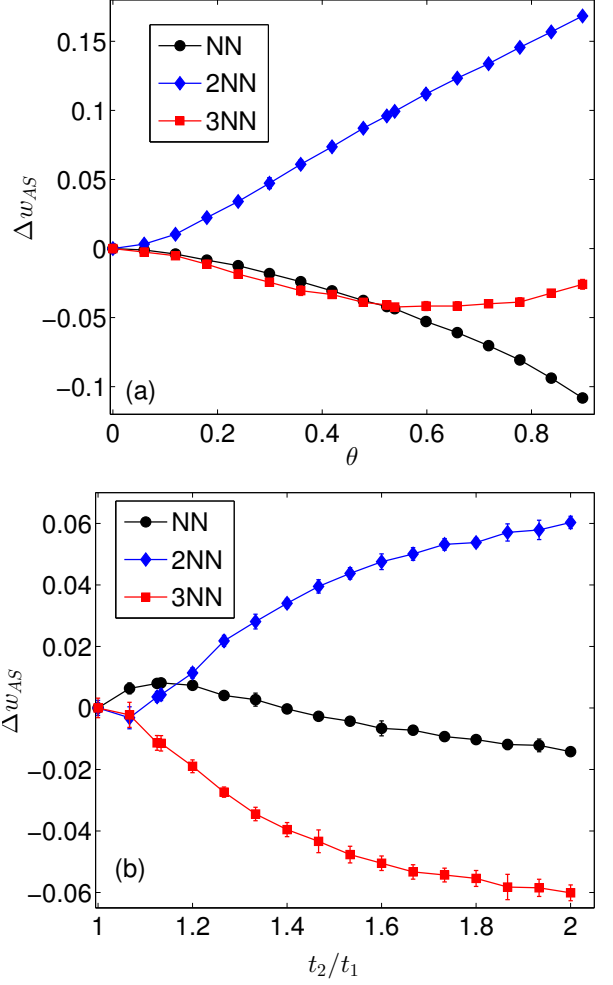


FIG. 4. θ and t_2/t_1 -dependent variations of total maximum anti-symmetric weights $\Delta w_{\text{AS}} = w_{\text{AS}} - w_{\text{AS}}^0$ for SU(3) CSL (a) and VBS (b), respectively, on NN, 2NN and 3NN bonds. VBS has the maximum w_{AS} on NN bonds at $t_2/t_1 = 1.125$ giving the variational energy $E_{\text{VBS}} = -0.4051(8)J_1$ per bond close to the tensor-network simulation.[35] We see that only an interaction on 2NN bonds can favor the SU(3) CSL.

with $\theta_1 = \theta_3 = -\theta_2/2 = \theta$ ($\theta_1 + \theta_2 + \theta_3 = 0$). The SPT state is protected by $\text{SU}(2) \times \text{U}(1)$. The components of 2-RDM, $|11\rangle\langle 11|$, $|13\rangle\langle 31|$, $|31\rangle\langle 13|$ and $|33\rangle\langle 33|$, have the SU(2) symmetry. There are four independent weights for 2-RDM, $\rho_{|11\rangle\langle 11|}$, $\rho_{|13\rangle\langle 31|}$, $\rho_{|22\rangle\langle 22|}$ and $\rho_{|23\rangle\langle 32|}$. The reference SU(3) DSL has the values

$$\begin{aligned} \rho_{|11\rangle\langle 11|}^0 &= 0.0509(3), & \rho_{|13\rangle\langle 31|}^0 &= -0.0904(5), \\ \rho_{|22\rangle\langle 22|}^0 &= 0.0508(2), & \rho_{|23\rangle\langle 32|}^0 &= -0.0902(6). \end{aligned}$$

Turning on θ , the variation of 2-RDM is defined by the

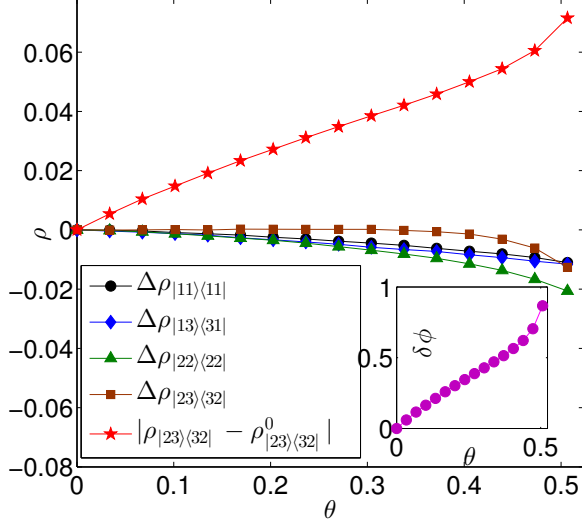


FIG. 5. The θ -dependence of variations of 2-RDM for the SPT state on NN bonds is defined in Eq. (9). The amplitude $|\rho_{|12><21|}$ varies little and phase $\delta\phi$ increase significantly for the small θ . GSH is potentially stabilized by twisted spin Hamiltonian in Eq. (10).

notations below

$$\begin{aligned}\Delta\rho_{|11><11|} &= -(\rho_{|11><11|} - \rho_{|11><11|}^0), \\ \Delta\rho_{|13><31|} &= -(\rho_{|13><31|} - \rho_{|13><31|}^0), \\ \Delta\rho_{|22><22|} &= -(\rho_{|22><22|} - \rho_{|22><22|}^0), \\ \Delta\rho_{|23><32|} &= |\rho_{|23><32|} - \rho_{|23><32|}^0|, \\ \delta\phi &= \arg(-\rho_{|23><32|}),\end{aligned}\quad (9)$$

where $\rho_{|23><32|} = -|\rho_{|23><32|}|e^{i\delta\phi}$ is complex.

The θ -dependent 2-RDM of SPT is shown in Fig. 5. We see that the absolute value $|\rho_{|23><32|}|$, and other $|\rho_{|ij><ij|}|$ vary little (< 0.02), however, the phase $\delta\phi \sim 1$ or $|\rho_{|23><32|} - \rho_{|23><32|}^0| \sim 0.1$. Such a large change in the phase of $\rho_{|23><32|}$ can be driven by the twisted permutation term on NN bonds

$$H^{SPT} = \sum_{\langle ij \rangle} P'_{ij}, \quad P'_{ij} = S_{\beta}^{\alpha}(i) S_{\alpha}^{\beta}(j) e^{i\Theta_{\alpha\beta}}, \quad (10)$$

which potentially stabilizes SPT state. Here $\Theta_{12} = \Theta_{32} = \Theta$, $\Theta_{13} = 0$ and $\Theta_{\alpha\beta} = -\Theta_{\beta\alpha}$ ($\alpha, \beta = 1, 2, 3$). We compare the VBS and SPT states for the twisted J_1 term and find that SPT will win when $\Theta > 0.6$. More systematic simulations (e.g. DMRG) are needed to confirm the result in further studies.

In conclusion, we start from Gutzwiller-projected parton wave functions to design supported local spin Hamiltonians. Gutzwiller projective parton construction is a powerful theoretical approach to construct many different wave function ansatzs with non-trivial topological properties. Our work establishes a rough directional

guide for further unbiased numerical simulations for these states.

We thank Zheng-Xin Liu, Peng Ye and Fang-Zhou Liu for helpful discussions. This research is supported by the BMO Financial Group and the John Templeton Foundation, and by NSF Grant No. DMR-1005541 and NSFC 11274192. Research at Perimeter Institute is supported by the Government of Canada through Industry Canada and by the Province of Ontario through the Ministry of Research.

-
- [1] M. Levin and X.-G. Wen, Phys. Rev. Lett. **96**, 110405 (2006).
 - [2] A. Kitaev and J. Preskill, Phys. Rev. Lett. **96**, 110404 (2006).
 - [3] X. Chen, Z.-C. Gu, and X.-G. Wen, Phys. Rev. B **82**, 155138 (2010).
 - [4] X. G. Wen, Phys. Rev. B **40**, 7387 (1989).
 - [5] F. Wilczek and A. Zee, Phys. Rev. Lett. **52**, 2111 (1984).
 - [6] X. G. Wen and Q. Niu, Phys. Rev. B **41**, 9377 (1990).
 - [7] X. G. Wen, International Journal of Modern Physics B **04**, 239 (1990).
 - [8] R. B. Laughlin, Phys. Rev. Lett. **50**, 1395 (1983).
 - [9] D. Arovas, J. R. Schrieffer, and F. Wilczek, Phys. Rev. Lett. **53**, 722 (1984).
 - [10] X. Chen, Z.-C. Gu, Z.-X. Liu, and X.-G. Wen, Science **338**, 1604 (2012).
 - [11] X.-L. Qi, Science **338**, 1550 (2012).
 - [12] X. Chen, Z.-C. Gu, Z.-X. Liu, and X.-G. Wen, Phys. Rev. B **87**, 155114 (2013).
 - [13] A. Kitaev, Annals of Physics **303**, 2 (2003).
 - [14] X.-G. Wen, Phys. Rev. Lett. **90**, 016803 (2003).
 - [15] M. A. Levin and X.-G. Wen, Phys. Rev. B **71**, 045110 (2005).
 - [16] A. Kitaev, Annals of Physics **321**, 2 (2006), january Special Issue.
 - [17] X. Chen, Z.-X. Liu, and X.-G. Wen, Phys. Rev. B **84**, 235141 (2011).
 - [18] K. Walker and Z. Wang, Frontiers of Physics **7**, 150 (2011).
 - [19] A. Läuscher and A. M. Läuchli, Phys. Rev. B **79**, 195102 (2009).
 - [20] F. Verstraete, V. Murg, and J. Cirac, Advances in Physics **57**, 143 (2008).
 - [21] E. Stoudenmire and S. R. White, Annual Review of Condensed Matter Physics **3**, 111 (2012).
 - [22] X. G. Wen, Phys. Rev. B **44**, 2664 (1991).
 - [23] X.-G. Wen, Phys. Rev. B **60**, 8827 (1999).
 - [24] P. Ye and X.-G. Wen, Phys. Rev. B **87**, 195128 (2013).
 - [25] Y.-M. Lu and D.-H. Lee, ArXiv e-prints (2012), arXiv:1212.0863 [cond-mat.str-el].
 - [26] I. Affleck, T. Kennedy, E. H. Lieb, and H. Tasaki, Phys. Rev. Lett. **59**, 799 (1987).
 - [27] I. Affleck and J. B. Marston, Phys. Rev. B **37**, 3774 (1988).
 - [28] P. A. Lee, N. Nagaosa, and X.-G. Wen, Rev. Mod. Phys. **78**, 17 (2006).
 - [29] Y. Ran, M. Hermele, P. A. Lee, and X.-G. Wen, Phys. Rev. Lett. **98**, 117205 (2007).

- [30] B. K. Clark, D. A. Abanin, and S. L. Sondhi, Phys. Rev. Lett. **107**, 087204 (2011).
- [31] A. F. Albuquerque, D. Schwandt, B. Hetényi, S. Capponi, M. Mambrini, and A. M. Läuchli, Phys. Rev. B **84**, 024406 (2011).
- [32] P. Corboz, M. Lajkó, A. M. Läuchli, K. Penc, and F. Mila, Phys. Rev. X **2**, 041013 (2012).
- [33] N. Trivedi and D. M. Ceperley, Phys. Rev. B **40**, 2737 (1989).
- [34] C. Waldtmann, H.-U. Everts, B. Bernu, C. Lhuillier, P. Sindzingre, P. Lecheminant, and L. Pierre, The European Physical Journal B - Condensed Matter and Complex Systems **2**, 501 (1998).
- [35] P. Corboz, K. Penc, F. Mila, and A. M. Läuchli, Phys. Rev. B **86**, 041106 (2012).
- [36] S.-S. Gong, W. Zhu, and D. N. Sheng, ArXiv e-prints (2013), arXiv:1312.4519 [cond-mat.str-el].
- [37] Y.-C. He, N. Sheng, D, and Y. Chen, Phys. Rev. Lett. **112**, 137202 (2014).
- [38] M. Hermele, Y. Ran, P. A. Lee, and X.-G. Wen, Phys. Rev. B **77**, 224413 (2008).
- [39] O. Cépas, C. M. Fong, P. W. Leung, and C. Lhuillier, Phys. Rev. B **78**, 140405 (2008).
- [40] P. Fazekas, *Lecture Notes on Electron Correlation and Magnetism*, Series in modern condensed matter physics (World Scientific, 1999).
- [41] Z.-X. Liu, Y. Zhou, H.-H. Tu, X.-G. Wen, and T.-K. Ng, Phys. Rev. B **85**, 195144 (2012).

SUPPLEMENTAL MATERIAL: MORE ON SPT

Given a twisted J_1 term

$$\begin{aligned}
 P'_{ij} S^{=1} = & \cos(\Theta)(\mathbf{S}_i \cdot \mathbf{S}_j + (\mathbf{S}_i \cdot \mathbf{S}_j)^2) + \sin(\Theta)\{[S_i^x(S_j^y S_j^z + S_j^z S_j^y) - (S_i^y S_i^z + S_i^z S_i^y)S_j^x] \\
 & - [S_i^y(S_j^x S_j^z + S_j^z S_j^x) - (S_i^x S_i^z + S_i^z S_i^x)S_j^y]\} + 2\sin^2(\Theta/2)[(S_i^x S_i^y + S_i^y S_i^x)(S_j^x S_j^y + S_j^y S_j^x) \\
 & + S_i^z S_j^z + ((S_i^x)^2 - (S_i^y)^2)((S_j^x)^2 - (S_j^y)^2) + \frac{1}{3}(2(S_i^z)^2 - (S_i^x)^2 - (S_i^y)^2)(2(S_j^z)^2 - (S_j^x)^2 - (S_j^y)^2)] \quad (11)
 \end{aligned}$$

we try to find the ground state in the vicinity of DSL state. We introduce two varational parameters, t_2/t_1 and θ , in our mean field Hamiltonian

$$H = - \sum_{\langle ij \rangle} t_{ij} e^{i\theta_\alpha} f_{i\alpha}^\dagger f_{j\alpha} + \text{h.c.}, \quad (12)$$

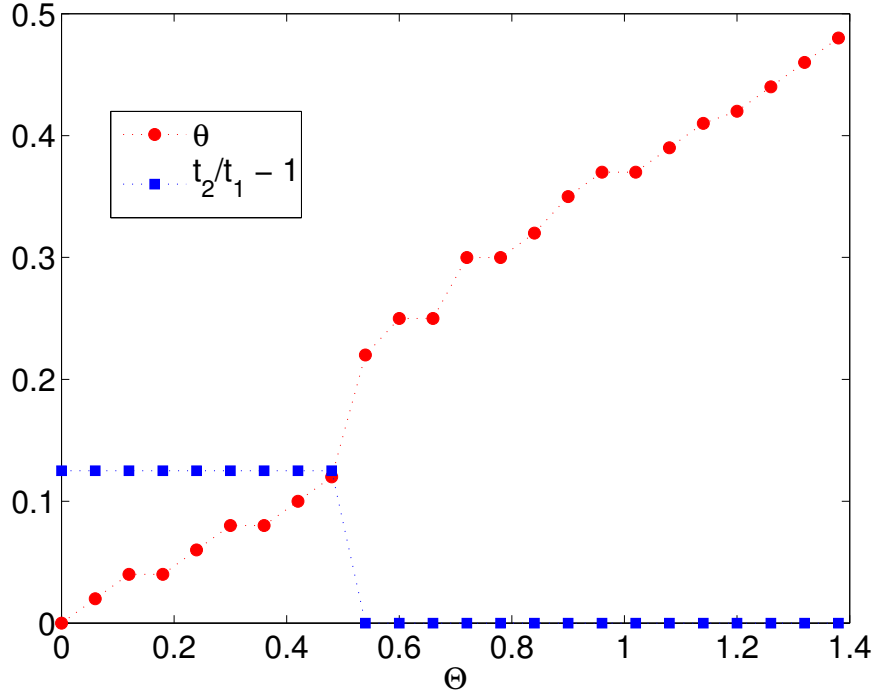


FIG. 6. The Θ dependence of optimized $t_2/t_1 - 1$ and θ .

When $\Theta < 0.55$, we always find the finite value of $t_2/t_1 - 1$ for the ground state. At the same time, the non-zero θ is also favored. When $\Theta > 0.55$, the uniform hopping amplitude is favored, $t_2/t_1 = 1$ and there is a jump of the slope for $\theta(\Theta)$.

To confirm the SPT state, we calculate the spin Hall conductance. The SPT state breaks $SU(3)$ symmetry into $SU(2) \otimes U(1)$ symmetry. We would like to show that the SPT state here is protected by two $U(1)$ symmetries, S_z and S_z^2 . The twisted Hamiltonian is indeed S_z and S_z^2 invariant. We would calculate the Hall response of SPT respect to S_z and S_z^2 $U(1)$ field. We need first to find out the charge assignment for the two different $U(1)$ field. Respect to $U(1)$ response, the mean field Hamiltonian should be written as

$$H = -t \sum_{\langle ij \rangle} e^{ia+iq_\alpha A} e^{i\theta_\alpha} f_{i\alpha}^\dagger f_{j\alpha} + \text{h.c.}, \quad (13)$$

where A is the external probe $U(1)$ field and a is the internal gauge field to enforce the single-occupation constraint. $\alpha = 1, 2, 3$ flavors have the different Chern number of the mean field filled bands, $C_1 = C_3 = -C_2 = 1$. The external A can generate the flavor current

$$J_\alpha = \frac{C_\alpha}{2\pi} (a + q_\alpha A), \quad (14)$$

To satisfy the single-occupation constraint, we have

$$\sum_\alpha J_\alpha = 0, \quad (15)$$

then we get

$$a = -\frac{\sum_\alpha C_\alpha q_\alpha}{\sum_\alpha C_\alpha} A \quad (16)$$

Therefore, the response mean field Hamiltonian is given as

$$H = -t \sum_{\langle ij \rangle} e^{iQ_\alpha A} e^{i\theta_\alpha} f_{i\alpha}^\dagger f_{j\alpha} + \text{h.c.} \quad (17)$$

with the effective charge respect to A , $Q_\alpha = q_\alpha - \frac{\sum_\alpha C_\alpha q_\alpha}{\sum_\alpha C_\alpha}$. For S_z , we get $\mathbf{q} = (1, 0, -1)$ and $\mathbf{Q} = (1, 0, -1)$. For S_z^2 , $\mathbf{q} = (1, 0, 1)$ and $\mathbf{Q} = (-1, -2, -1)$. All the charges are integers. Therefore there is no ground state degeneracy. To see this clearly, we can also calculate S_z and S_z^2 charges for chiral spin liquid state. For CSL, $\mathbf{Q} = (1, 0, -1)$ for S_z and $\mathbf{Q} = (\frac{1}{3}, -\frac{2}{3}, \frac{1}{3})$ for S_z^2 . From the charge fractionalization, we know CSL has the three-fold ground state degeneracy.

To calculate the spin Hall conductance, we impose the general twisted boundary phase on the system

$$f_{i+L_x\alpha} = f_{i\alpha} e^{iQ_\alpha \phi_x}, \quad f_{i+L_y\alpha} = f_{i\alpha} e^{iQ_\alpha \phi_y}. \quad (18)$$

From the response mean field Hamiltonian, we can obtain the response Gutzwiller-projected wave function. The spin Hall conductance is given as

$$\sigma_s = \frac{1}{2\pi} \int_{-\pi}^{\pi} d\phi_x \int_{-\pi}^{\pi} d\phi_y \Omega(\phi_x, \phi_y) \quad (19)$$

with the Berry curvature

$$\Omega(\phi_x, \phi_y) = \nabla \times \langle \Psi_G | i \nabla_\phi | \Psi_G \rangle \quad (20)$$

Numerically, we divide the unit cell of the boundary phases into 8-by-8 mesh points. The spin Hall conductance is given as

$$\sigma_s = \frac{1}{2\pi} \sum_j \Omega_j \quad (21)$$

with Berry curvature

$$\Omega_j = \arg \prod_i \langle \Psi_G^{j+1} | \Psi_G^j \rangle, \quad (22)$$

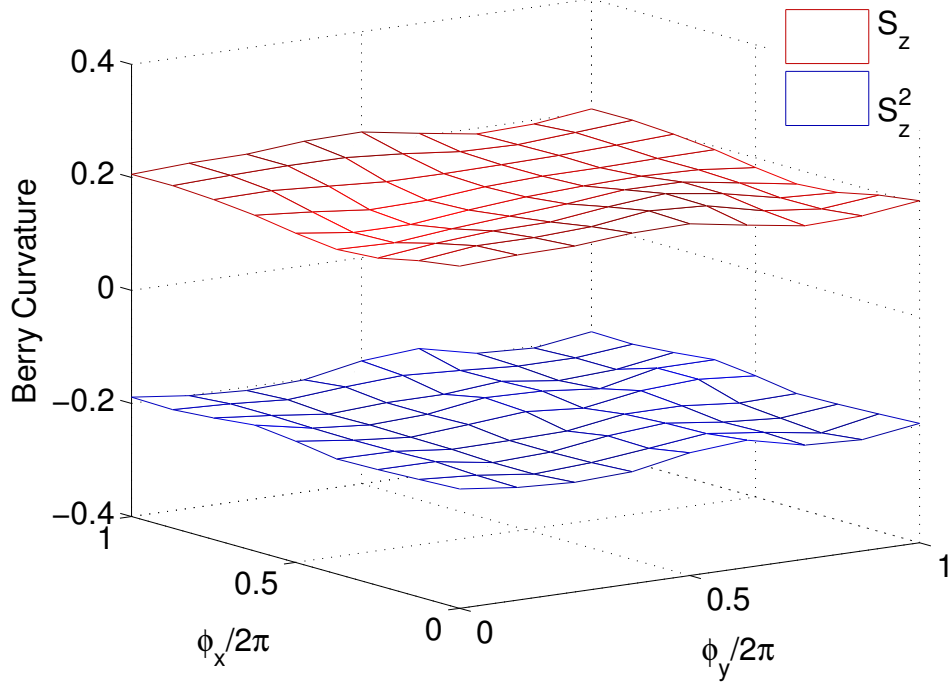


FIG. 7. The spin Berry curvature for S_z and S_z^2 for SPT state.

where $i = 1 - 4$ (with $j_5 \equiv j_1$) denote four mesh points at the j -th plaquette of the k mesh patches. The Gutzwiller projected wavefunctions can be written as

$$|\Psi\rangle = \sum_{R_i} \psi(R_i) |R_i\rangle \quad (23)$$

with

$$\psi(R_i) = \det(\varphi_i(\mathbf{r}_i)) \quad (24)$$

On the k mesh, we need calculate $2N_k$ overlap of the wavefunctions

$$\begin{aligned} \frac{\langle \Psi_j | \Psi_{j'} \rangle}{\langle \Psi_j | \Psi_j \rangle} &= \frac{\sum_{R_i} \psi_j^*(R_i) \psi_{j'}(R_i)}{\sum_{R_i} |\psi_j(R_i)|^2} \\ &= \frac{\sum_{R_i} |\psi_j(R_i)|^2 \frac{\psi_{j'}(R_i)}{\psi_j(R_i)}}{\sum_{R_i} |\psi_j(R_i)|^2} \end{aligned} \quad (25)$$

where the summation can be done with the standard VMC technique with the weight $|\psi_j(R_i)|^2$. To calculate the berry curvature, we need calculate $2N_k$ overlap of the wavefunctions with different boundary condition \mathbf{k} . Thus we will take the weight

$$\rho(R_i) = \sum_k |\psi_k(R_i)|^2 \quad (26)$$

and the overlap is calculated as

$$\begin{aligned} \frac{\langle \Psi_j | \Psi_{j'} \rangle}{\sum_{R_i} \rho(R_i)} &= \frac{\sum_{R_i} \psi_j^*(R_i) \psi_{j'}(R_i)}{\sum_{R_i} \rho(R_i)} \\ &= \frac{\sum_{R_i} \rho(R_i) \frac{\psi_j^*(R_i) \psi_{j'}(R_i)}{\rho(R_i)}}{\sum_{R_i} \rho(R_i)} \end{aligned} \quad (27)$$

The spin Berry curvature respect to S_z and S_z^2 for SPT are shown in Fig. 7. The spin Hall conductance is $\sigma_s(S_z) = 2$ and $\sigma_s(S_z^2) = -2$. It is the same as the results from K -matrix methods.